CrystEngComm

Accepted Manuscript

This is an *Accepted Manuscript*, which has been through the Royal Society of Chemistry peer review process and has been accepted for publication.

Accepted Manuscripts are published online shortly after acceptance, before technical editing, formatting and proof reading. Using this free service, authors can make their results available to the community, in citable form, before we publish the edited article. We will replace this *Accepted Manuscript* with the edited and formatted *Advance Article* as soon as it is available.

You can find more information about *Accepted Manuscripts* in the Information for Authors.

Please note that technical editing may introduce minor changes to the text and/or graphics, which may alter content. The journal's standard Terms & Conditions and the Ethical guidelines still apply. In no event shall the Royal Society of Chemistry be held responsible for any errors or omissions in this *Accepted Manuscript* or any consequences arising from the use of any information it contains.

ROYAL SOCIETY OF CHEMISTRY

www.rsc.org/crystengcomm

Cite this: DOI: 10.1039/c0xx00000x

www.rsc.org/xxxxxx

ARTICLE TYPE

Polycarboxylate-directed various Co(II) complexes based on a "V"-like bis-pyridyl-bis-amide derivative: Construction, electrochemical and photocatalytic properties †

Xiu-Li Wang*, Xiao-Ting Sha, Guo-Cheng Liu, Nai-Li Chen and Yuan Tian

Received (in XXX, XXX) Xth XXXXXXXXX 20XX, Accepted Xth XXXXXXXXX 20XX
DOI: 10.1039/b000000x

A series of new Co(II) complexes based on a new semi-rigid "V"-like bis-pyridyl-bis-amide derivative, namely, $[Co(3\text{-bpha})_2(2,3\text{-HPDC})_2]$ (**1**), $[Co(3\text{-bpha})(3\text{-NPH})(H_2O)_2]\cdot 2H_2O$ (**2**), $[Co(3\text{-bpha})(1,3\text{-BDC})]\cdot 4H_2O$ (**3**), $[Co(3\text{-bpha})(HIP)]\cdot 3H_2O$ (**4**), $[Co(3\text{-bpha})(MIP)(H_2O)]\cdot H_2O$ (**5**), $[Co_3(3\text{-bpha})_2(1,3,5\text{-BTC})_2(H_2O)_4]\cdot 2H_2O$ (**6**) (3-bpha = N,N′-bis(pyridin-3-yl)-5-hydroxybenzene-1,3-dicarboxamide, 2,3-H_2PDC = 2,3-pyridinedicarboxylic acid, 3-H_2NPH = 3-nitrophthalic acid, 1,3-H_2BDC = 1,3-benzenedicarboxylic acid, H_2HIP = 5-hydroxyisophthalic acid, H_2MIP = 5-methylisophthalic acid, 1,3,5-H_3BTC = 1,3,5-benzenetricarboxylic acid), have been hydrothermally synthesized by tuning aromatic polycarboxylates co-ligands and characterized by single-crystal X-ray diffraction, IR spectra, powder XRD and TG analysis. Complex **1** is a discrete zero-dimensional (0D) structure, in which the 3-bpha ligands and the 2,3-HPDC anions act as the terminal groups simultaneously to coordinate with the Co^{II} ions. Complex **2** is a 1D meso-helical chain, in which the 3-bpha ligands show a μ_2-bridging mode and the 3-NPH anions act as the terminal groups. In complexes **3** and **4**, pairs of 3-bpha ligands integrate with two Co^{II} ions to generate 28-membered $Co_2(3\text{-bpha})_2$ rings, which connect with the 1D $[Co\text{-}1,3\text{-BDC}]_n$ or $[Co\text{-HIP}]_n$ chains to create the 2D networks. In complex **5**, the Co^{II} ions are linked by 3-bpha ligands resulting in a single-strand $[Co\text{-}3\text{-bpha}]_n$ helix chain, which is further connected by the MIP anions to form a 2D network. Complex **6** show a 3D framework with (3,3,4)-connected $(8^3)_4(8^4\cdot 10^2)$ topology, which contains $[Co\text{-}(1,3,5\text{-BTC})]_n$ 2D grid-like sheets and 1D $[Co\text{-}3\text{-bpha}]_n$ helical chains. Finally, the 0D discrete architecture in **1**, 1D chain in **2**, 2D networks in **4** and **5** are extended to 3D supramolecular frameworks through hydrogen bonding interactions. The effect of polycarboxylates auxiliary ligands with different substitute groups, different carboxyl positions and number on the assembly and structures of the target complexes were discussed. Moreover, the thermal stabilities, electrochemical properties and photocatalytic activities of complexes **1**–**6** were investigated.

Introduction

The rational design and construction of novel metal–organic coordination polymers (MOCPs) is currently attracting considerable attention, not only because of their fascinating topological structures, but also due to their potential applications in the fields of catalysis, luminescence, gas adsorption, nonlinear optics and magnetic materials.[1] It is well-known that several factors have effects on the formation of the final structures, such as organic ligands, geometric requirement of the metal ions, the reaction time, temperature, pH, solvent system and so on.[2] Among these factors, the organic ligands as the structure connectors play the most important role in the whole frameworks of MOCPs.[3] Therefore, significant interest has arisen in the structural tuning of coordination polymers through rational design and selection of organic ligands containing N/O-donor. Among various N/O-donor ligands, bis-pyridyl-bis-amide and their derivatives as a kind of excellent organic ligands with the unique potential to provide two types of hydrogen bonding sites, the –NH moieties acting as electron acceptors and the –C=O groups acting as electron donors, are now receiving extensive attention.[4]

On the other hand, organic polycarboxylates as a kind of multidentate O-donor ligands are excellent building blocks with versatile coordination modes for constructing metal-organic frameworks with interesting structures and properties.[5] Therefore, the combination of pyridyl-amide-based ligands and

Department of Chemistry, Bohai University, Liaoning Province Silicon Materials Engineering Technology Research Centre, Jinzhou, 121000, P. R. China Fax: +86-416-3400158; Tel: +86-416-3400158; Email: wangxiuli@bhu.edu.cn

††Electronic Supplementary Information (ESI) available: IR, TG, PXRD and additional figures. CCDC 1404928, 1404929, 1404930, 1404931, 1404932 and 1404933. For ESI and crystallographic data in CIF or other electronic format see DOI: 10.1039/b000000x

CrystEngComm Accepted Manuscript

polycarboxylate ligands can be regarded as an effective strategy to prepare attractive metal–organic coordination frameworks with different dimensionalities, which attracted great interest from researchers.[6] We also devoted our efforts to the synthesis of carboxylate-assisted pyridyl-acylamide-based coordination polymers with diverse structures and functions.[7] However, reports on the combination of semi-rigid bis-pyridyl-bis-amide derivatives and organic polycarboxylates with different substitute groups and carboxyl groups are still limited.[8] So in this work, we designed a semi-rigid "V"-shaped N,N′-bis(pyridin-3-yl)-5-hydroxybenzene-1,3-dicarboxamide (3-bpha) as the main ligand to construct target complexes, which has not been used in the construction of complexes according to CCDC database. In order to explore the effect of substitute groups as well as carboxyl position and number of ploycarboxylates on the structures of target complexes, six types of aromatic polycarboxylates, namely, 2,3-pyridinedicarboxylic acid (2,3-H_2PDC), 3-nitrophthalic acid (3-H_2NPH), 1,3-benzenedicarboxylic acid (1,3-H_2BDC), 5-hydroxyisophthalic acid (H_2HIP), 5-methylisophthalic acid (H_2MIP) and 1,3,5-benzenetricarboxylic acid (1,3,5-H_3BTC) were selected as the co-ligands to combine with the "V"-shaped pyridyl-formamide derivative 3-bpha for constructing the target complexes. The different substitute groups and carboxyl groups for these ligands may be favorable to generate novel architectures.

The Co^{II} ions are the most commonly reported metals and show excellent electrochemical properties when coordinated by multidentate ligands.[9] In addition, photocatalysts have attracted much attention because of their potential applications in purifying waste water by thoroughly decomposing organic pollutants. Some transition metal complexes have been proved to be efficient photocatalysts on the degradation of organic dyes.[10, 7a] However, reports on Co^{II}-based CPs photocatalysts are still very limited.

Herein six new Co^{II} complexes, namely, [Co(3-bpha)$_2$(2,3-HPDC)$_2$] (**1**), [Co(3-bpha)(3-NPH)(H_2O)$_2$]·2H_2O (**2**), [Co(3-bpha)(1,3-BDC)]·4H_2O (**3**), [Co(3-bpha)(HIP)]·3H_2O (**4**), [Co(3-bpha)(MIP)(H_2O)]·H_2O (**5**), [Co_3(3-bpha)$_2$(1,3,5-BTC)$_2$(H_2O)$_4$]·2H_2O (**6**) were obtained under hydrothermal conditions. The effect of polycarboxylates auxiliary ligands on the assembly and structures of the title complexes was discussed. In addition, the photocatalytic activities and the electrochemical properties of complexes **1**–**6** were investigated.

Experimental section

Materials and methods

Materials and characterization. All chemicals were of reagent grade, and used without further purification. Ligand 3-bpha was synthesized according to the literature method.[11] FT-IR spectra (KBr pellets) were taken on a Varian-640 spectrometer. Thermogravimetric analyses (TGA) were recorded on a Pyris Diamond TG instrument. Powder X-ray diffraction (PXRD) investigations were carried out with a Ultima IV with D/teX Ultra diffractometer at 40 kV, 40 mA with Cu-Kα (λ = 1.5406 Å) radiation. Electrochemical measurements were carried out on a CHI 440 electrochemical workstation. A conventional three-electrode system was used at room temperature. The title complexes chemically bulk-modified carbon paste electrodes (CPEs) were used as the working electrodes. A saturated calomel electrode (SCE) and a platinum wire were used as the reference and auxiliary electrodes, respectively. UV-Vis absorption spectra were obtained using a SP-1901 UV-Vis spectrophotometer.

Preparation of complexes 1 – 6

Synthesis of [Co(3-bpha)$_2$(2,3-HPDC)$_2$] (1). A mixture containing $CoCl_2·6H_2O$ (0.048 g, 0.2 mmol), 3-bpha (0.033 g, 0.10 mmol), 2,3-H_2PDC (0.034 g, 0.20 mmol), NaOH (0.016 g, 0.40 mmol) and H_2O (12 mL) was placed in a 25 mL Teflon-lined autoclave and heated to 120 °C for 4 days under autogenous pressure. Then it was allowed to cool to room temperature, yellow block crystals of **1** suitable for X-ray diffraction could be isolated in about 16% yield (based on Co). IR (KBr, cm^{-1}): 3275w, 3140w, 3076w, 2358w, 1656s, 1583s, 1543s, 1425s, 1354s, 1278m, 1230s, 1101s, 1056w, 981m, 885s, 810s, 746m, 719s, 667s, 599m, 561m, 516m.

Synthesis of [Co(3-bpha)(3-NPH)(H_2O)$_2$]·2H_2O (2). Complex **2** was prepared in the same way as **1** except that 3-H_2NPH (0.042 g, 0.20 mmol) was used instead of 2,3-H_2PDC. Pink crystals of **2** suitable for X-ray diffraction were isolated in about 40% yield (based on Co). IR (KBr, cm^{-1}): 3344w, 2362w, 1668m, 1589s, 1552s, 1489m, 1463m, 1428s, 1396s, 1342s, 1282w, 1222m, 1134w, 1055m, 1001m, 927m, 893m, 815s, 700s, 642m.

Synthesis of [Co(3-bpha)(1,3-BDC)]·4H_2O (3). The synthetic procedure for **3** was the same as for **1**, except that 1,3-H_2BDC (0.033 g, 0.20 mmol) was used instead of 2,3-H_2PDC. Purple crystals of **3** were obtained in a yield of about 20% based on Co. IR (KBr, cm^{-1}): 3429w, 3282w, 3066w, 2360w, 1654m, 1618s, 1550s, 1485s, 1392s, 1334m, 1292s, 1219s, 1112w, 1055w, 999w, 920w, 815m, 752s, 721m, 669w, 601w.

Synthesis of [Co(3-bpha)(HIP)]·3H_2O (4). Synthesis of **4** was similar to that of **1** except that H_2HIP (0.036 g, 0.20 mmol) was used instead of 2,3-H_2PDC. Purple block crystals of **4** were obtained in a 32% yield based on Co. IR (KBr, cm^{-1}): 3344w, 3072w, 2362w, 1660s, 1577s, 1537s, 1421s, 1344m, 1276m, 1240m, 1109m, 1053w, 981m, 883s, 786s, 731s, 698s, 646w, 594w.

Synthesis of [Co(3-bpha)(MIP)(H_2O)]·H_2O (5). The synthetic procedure for **5** was similar to that of **1** except that H_2MIP (0.036 g, 0.20 mmol) was used instead of 2,3-H_2PDC. Light pink crystals of **5** suitable for X-ray diffraction were isolated in about 35% yield (based on Co). IR (KBr, cm^{-1}): 3421w, 2362w, 1676w, 1610m, 1544s, 1483s, 1427s, 1375s, 1338s, 1288m, 1232m, 1112w, 1053w, 999w, 810s, 775s, 702s, 597w.

Synthesis of [Co_3(3-bpha)$_2$(1,3,5-BTC)$_2$(H_2O)$_4$]·2H_2O (6). The preparation of complex **6** was the same as for **1,** except that 1,3,5-H_3BTC (0.042 g, 0.2 mmol) was used instead of 2,3-H_2PDC and different amount of NaOH (0.024 g, 0.60 mmol). Purple crystals of **6** were obtained in a yield of about 22% based on Co. IR (KBr, cm^{-1}): 3246w, 2360w, 1670m, 1633s, 1583s, 1427s, 1371s, 1280m, 1236w, 1101w, 885w, 796m, 732s, 700m, 669w, 536w.

Preparation of complexes 1–6 bulk-modified CPEs

CrystEngComm Accepted Manuscript

This journal is © The Royal Society of Chemistry [year]

Complex **1** bulk-modified carbon paste electrode (**1**-CPE) was fabricated as follows: 0.10 g graphite powder and 0.010 g complex **1** were mixed and ground together by the agate mortar and pestle to achieve an even mixture, and then 0.05 mL of Nujol was added with stirring. The homogenized mixture was packed into a glass tube with 3 mm inner diameter to a length of 8 mm, and the tube surface was wiped with weighing paper. The electrical contact was established with the copper wire.[12] The same procedure was used for the preparation of bare CPE and **2**–**6**-CPEs.

X-ray crystallography

Diffraction data for complexes **1**–**6** were collected on a Bruker SMART APEX II diffractometer equipped with a CCD area detector and graphite-monochromated Mo-K_α (λ = 0.71073 A°) by using the φ-ω scan technique at 296(2) K. The structures were solved by direct methods using the program *SHELXS* and refined anisotropically on F^2 by the fullmatrix least-squares technique using the *SHELXL* crystallographic software package.[13] For the title complexes, all non-hydrogen atoms were refined anisotropically, the hydrogen atoms of the organic ligands were generated theoretically onto the specific atoms and refined isotropically with fixed thermal factors. O4W of complex **2** was restricted by the 'isor' command and the distances between H3WB and H8A in complex **4** and N3 and H3B in complex **6** were restricted by 'dfix' command. In addition, the unit cell of complex **6** includes a large region of disordered solvent water molecules, which could not be modeled as discrete atomic sites. Thus, the SQUEEZE program[14] was used to further estimate the number of solvent water molecules in the crystal structure. When the electron density and TGA are taken into account, two water molecules are determined. The crystal data and structure refinement results for complexes **1**–**6** are summarized in Table 1. Selected bond distances and bond angles are listed in Tables S1–S6. Crystallographic data for the structures reported in this paper have been deposited in the Cambridge Crystallographic Data Center with CCDC numbers 1404928, 1404929, 1404930, 1404931, 1404932 and 1404933.

Table 1 Crystallographic data for complexes **1-6**.

Complex	**1**	**2**	**3**	**4**	**5**	**6**
Formula	$C_{50}H_{36}CoN_{10}O_{14}$	$C_{26}H_{25}CoN_5O_{13}$	$C_{26}H_{26}CoN_4O_{11}$	$C_{26}H_{24}CoN_4O_{11}$	$C_{27}H_{23}CoN_4O_9$	$C_{54}H_{46}Co_3N_8O_{24}$
Formula wt.	1059.82	674.44	629.44	627.42	606.42	1367.78
Crystal system	Triclinic	Monoclinic	Triclinic	Triclinic	Monoclinic	Orthorhombic
Space group	*P*-1	*P*2(1)/*n*	*P*-1	*P*-1	*P*2(1)/*c*	*Pbcn*
T (K)	296(2)	296(2)	296(2)	296(2)	296(2)	296(2)
a (Å)	8.6580(6)	7.2427(4)	10.0924(6)	10.0129(19)	9.9555(6)	12.6867(7)
b (Å)	10.2661(7)	25.0077(14)	11.0595(7)	10.724(2)	16.4810(10)	27.5595(15)
c (Å)	13.9044(9)	15.4019(8)	13.9619(8)	13.961(3)	16.1393(10)	15.8184(8)
α (°)	76.2120(10)	90	66.8310(10)	73.385(3)	90	90
β (°)	72.9620(10)	99.4770(10)	83.4210(10)	73.609(4)	100.6730(10)	90
γ (°)	72.0970(10)	90	71.2790(10)	64.888(3)	90	90
V (Å ^{3})	1109.39(13)	2751.6(3)	1356.78(14)	1278.2(4)	2602.3(3)	5530.7(5)
Z	1	4	2	2	4	4
D_{calc} (g/cm^3)	1.586	1.628	1.541	1.630	1.548	1.643
μ/mm^{-1}	0.474	0.704	0.702	0.745	0.723	0.985
F(000)	545	1388	650	646	1248	2796
θ_{max} (°)	28.30	28.01	28.36	28.31	24.95	25.00
R_{int}	0.0114	0.0314	0.0205	0.0313	0.0315	0.0765
$R_1{}^a$ [I>2σ(I)]	0.0342	0.0559	0.0413	0.0685	0.0384	0.0783
$wR_2{}^b$(all data)	0.1007	0.1631	0.1084	0.2136	0.1046	0.1676
GOF	1.000	1.000	1.000	1.000	1.000	1.001
$\Delta\rho_{max}$(e Å^{-3})	0.566	2.312	0.513	2.681	0.439	0.741
$\Delta\rho_{min}$(e Å^{-3})	-0.518	-1.560	-0.402	-0.852	-0.465	-0.674

$^a R_1 = \Sigma||F_o|-|F_c||/\Sigma|F_o|$; $^b wR_2 = \Sigma[w(F_o^2-F_c^2)^2]/\Sigma[w(F_o^2)^2]^{1/2}$

Results and discussion

Description of crystal structures

[Co(3-bpha)$_2$(2,3-HPDC)$_2$] (1). Single crystal X-ray diffraction analysis reveals that complex **1** crystallizes in the triclinic space group *P*-1. The crystal structure of complex **1** contains a Co^{II} cation, two 3-bpha ligands and two 2,3-HPDC anions. As shown in Fig. 1a, each Co^{II} ion with a {CoN_4O_2} octahedral coordination geometry is six-coordinated by four pyridyl nitrogen atoms from two 3-bpha ligands and two 2,3-HPDC anions, respectively [Co(1)–N(1) = Co(1)–N(1)#1 = 2.164(13) Å, Co(1)–N(5) = Co(1)–N(5)#1 = 2.116(13) Å], and

CrystEngComm Accepted Manuscript

two oxygen atoms of two carboxyl groups from two 2,3-HPDC anions [Co(1)–O(1) = Co(1)–O(1)#1 = 2.088(11) Å].

In complex **1**, both 3-bpha and 2,3-HPDC ligands show one type of coordination mode. Two 3-bpha and two 2,3-HPDC ligands act as terminal groups coordinating with Co^{II} ion to form a 0D complex $[Co(3\text{-bpha})_2(2,3\text{-HPDC})_2]$. These discrete complexes are connected together by the hydrogen bonding interactions between the oxygen atoms of 2,3-HPDC anions and the nitrogen atoms of 3-bpha ligands [O(4)–H(4A)···N(4), O···N = 2.596(1) Å] to form a 1D supramolecular chain (Fig. 1b). The adjacent 1D chains are linked together by the hydrogen bonding interactions between the nitrogen atoms of 3-bpha ligands and the oxygen atoms of 2,3-HPDC anions [N(2)–H(2B)···O (3), N···O = 2.864(2) Å] to construct a 2D supramolecular net (Fig. S1a). The final 3D supramolecular framework of complex **1** is generated also through the hydrogen bonding interactions between the carbon atoms of 2,3-HPDC anions and oxygen atoms from 3-bpha ligands [C(23)–H(23A)···O(6), C···O = 3.246(6) Å] (Fig. S1b). Generally speaking, semi-rigid bis-pyridyl-bis-amide ligands and other polycarboxylates mixed ligands exhibit bridging coordination modes, such as $[Zn(bppdca)(BDC)]\cdot H_2O$ [8b] and $[Cd(MEDPQ)(2,3\text{-PDC})]_n$.[15] While in complex **1**, 3-bpha and 2,3-HPDC anions act as the terminal groups simultaneously, which is rarely reported to the best of our knowledge.

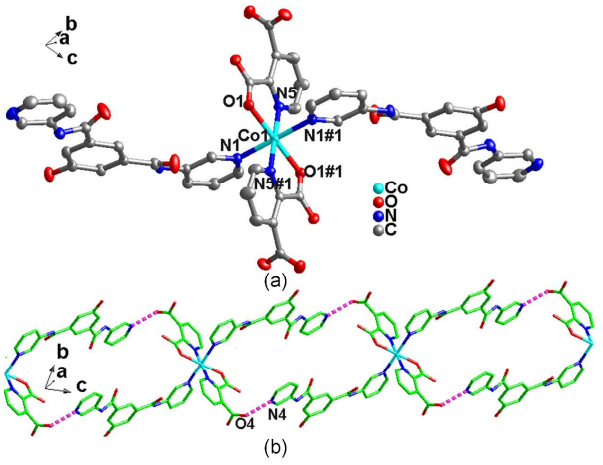

Fig. 1 (a) The coordination environment of the Co^{II} ion in complex **1**. (#1 $-x + 1, -y + 1, -z$); (b) 1D supramolecular chain of **1** extended by hydrogen bonding interactions. The hydrogen atoms are omitted for clarity.

$[Co(3\text{-bpha})(3\text{-NPH})(H_2O)_2]\cdot 2H_2O$ (2). X-ray diffraction analysis reveals that complex **2** crystallizes in the monoclinic space group $P2(1)/n$. **2** consists of one Co^{II} ion, one 3-bpha ligand, one 3-NPH anion, two coordinated water molecules and two lattice water molecules. As show in Fig. 2a, each Co^{II} ion is six-coordinated by two pyridyl nitrogen atoms from two individual 3-bpha ligands [Co(1)–N(1) = 2.165(3) Å, Co(1)–N(4)#1 = 2.197(3)], two oxygen atoms from two carboxyl groups of one 3-NPH anion and two coordinated water molecules with the Co–O distances from 2.072(2) to 2.132(2) Å, forming a distorted octahedral geometry $\{CoN_2O_4\}$.

In complex **2**, each 3-bpha as a bidentate ligand with a μ_2-bridging mode connects the adjacent Co^{II} ions to form a 1D $[Co\text{-}3\text{-bpha}]_n$ meso-helical chain, in which the Co···Co separation is 12.618 Å (Fig. 2b). In addition, two carboxyl groups of each 3-NPH anion show a μ_1-η^1:η^1 chelating coordination mode and coordinate with one Co^{II} ion as terminal groups. The adjacent 1D chains are extended into 2D supramolecular network by the hydrogen bonding interactions between the oxygen atoms from 3-bpha ligands and 3-NPH anions [O(8)–H(8B)···O(2), O···O = 2.692(1) Å] (Fig. 2c). The final 3D supramolecular framework of complex **2** is formed also through the hydrogen bonding interactions between the oxygen atoms from lattice water molecules and 3-bpha ligands, respectively [O(2W)–H(2WB)···O(3), O···O = 2.670(7) Å] (Fig. S2). In our previous studies, we have used 3-NPH anions as the secondary ligand combining with flexible bis-pyridyl-bis-amide ligands to construct complexes, such as $[Cu(3\text{-dpyh})(3\text{-NPH})(H_2O)_2]$, $[Ni(3\text{-dpyh})(3\text{-NPH})(H_2O)_2]$ and $[Co(3\text{-dpyh})(3\text{-NPH})(H_2O)_2]$.[16] In those complexes, 3-NPH exhibits bridging coordination mode. In complex **2**, 3-NPH anions act as the terminal groups, which is different from the above complexes.

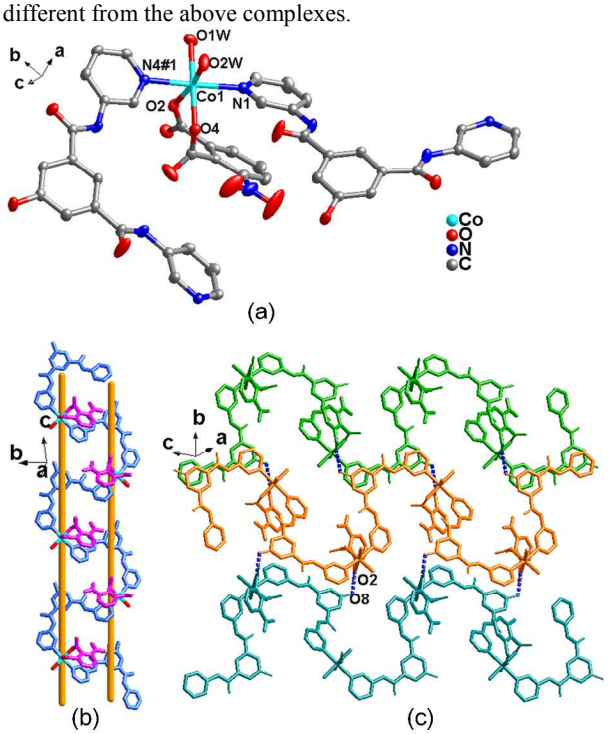

Fig. 2 (a) Coordination environment of the Co^{II} ion in **2** (#1 $x - 1/2, -y + 1/2, z + 1/2$); (b) The 1D meso-helical chain of **2**; (c) The 2D supramolecular network extended by hydrogen bonding interactions. The hydrogen atoms are omitted for clarity.

$[Co(3\text{-bpha})(1,3\text{-BDC})]\cdot 4H_2O$ (3) and $[Co(3\text{-bpha})(HIP)]\cdot 3H_2O$ (4). Structural analyses indicate that the final networks of complexes **3** and **4** are very similar, as shown in Fig. 3 and Fig. S3, so complex **3** is taken as a representative example for detailed structural description. Single crystal X-ray diffraction analysis reveals that **3** crystallizes in the triclinic system with space group P-1. Complex **3** consists of one Co^{II} ion, one 3-bpha ligand, one 1,3-BDC anion and four lattice water molecules. As depicted in Fig. 3a, the coordination environment around the Co^{II} ion is composed of two nitrogen atoms from two 3-bpha ligands [Co(1)–N(1) = 2.152(19) Å, Co(1)–N(4)#3 = 2.185(19) Å] and four oxygen atoms of three carboxyl groups from three 1,3-BDC anions with the Co–O distances from 2.005(15) to 2.418(15) Å, showing a distorted octahedral geometry $\{CoN_2O_4\}$.

CrystEngComm Accepted Manuscript

This journal is © The Royal Society of Chemistry [year]

In complex **3**, two 3-bpha ligands in the *anti*-configuration integrate with two Co^{II} ions to generate a 28-membered Co_2(3-bpha)$_2$ ring. The carboxyl groups of 1,3-BDC possess two different coordination modes: bidentate bridging coordination mode and chelate coordination mode. It is noted that all the carboxylic oxygen atoms from the 1,3-BDC carboxylate coordinate with the Co^{II} ions, forming an infinite 1D [Co-1,3-BDC]$_n$ ladder-like double chain. The adjacent 1D chains are linked by the 28-membered Co_2(3-bpha)$_2$ loops to form an intricate 2D network (Fig. 3b). In order to simplify the structure of complex **3**, each Co^{II}, 1,3-BDC anion and 3-bpha ligand can be defined as 5-, 3- and 2-connected nodes, respectively. Thus, the 2D structure of complex **3** can be described as a (2,3,5)-connected network with $(4^2\cdot6)(4^3\cdot6\cdot8^4\cdot10^2)(4)$ topology (Fig. 3c). There are no appropriate hydrogen-bonding interactions in **3**. While in **4**, the 2D networks are extended to 3D supramolecular framework through the hydrogen bonding interactions between the oxygen atoms of 3-bpha ligands and oxygen atoms from the carboxyl group of HIP anions and lattice water molecules, respectively [O(5)–H(5B)···O(1W), O···O = 2.786(8) Å, O(1W)–H(1WB)···O(2), O···O = 2.810(7) Å] (Fig. S3).

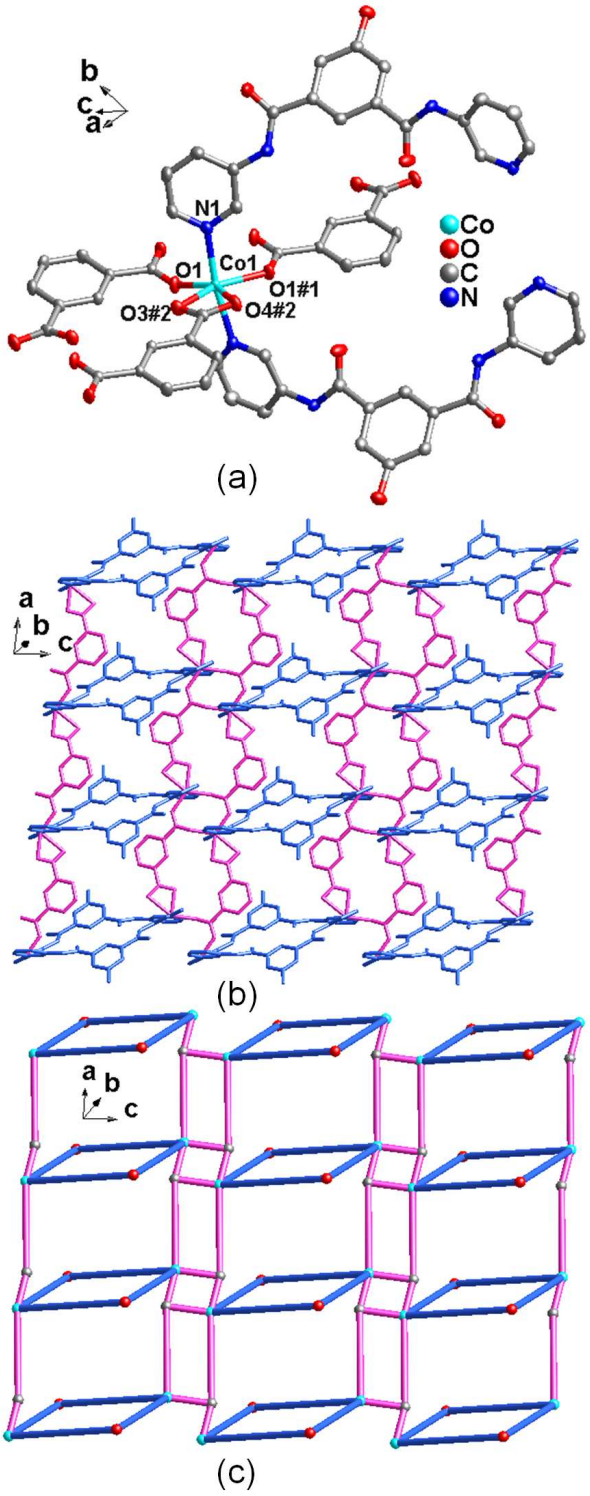

Fig. 3 (a) Coordination environment of the Co^{II} ion in **3** (#1 $-x, -y+1, -z+2$; #2 $-x+1, -y+1, -z+2$); (b) The 2D network of **3**; (c) The 2D topology with $(4^2\cdot6)(4^3\cdot6\cdot8^4\cdot10^2)(4)$. The hydrogen atoms are omitted for clarity.

[Co(3-bpha)(MIP)(H$_2$O)]·H$_2$O (5). Single-crystal X-ray diffraction analysis reveals that complex **5** crystallizes in the monoclinic space group *P*2(1)/*c*. In the coordination environment of **5**, there is one crystallographically independent Co^{II} center, one 3-bpha ligand, one MIP anion, one coordinated water molecule and one lattice water molecule. The Co^{II} center is six-coordinated by two pyridyl N atoms from two 3-bpha ligands [Co(1)–N(1) = 2.093(2) Å, Co(1)–N(4)#2 = 2.124(2) Å] and four O atoms from two MIP anions and one coordinated water molecule, respectively [Co–O = 2.019(18)–2.161(2) Å], which adopts an octahedral {CoN_2O_4} coordination geometry (Fig. 4a).

In complex **5**, the μ_2-bridging 3-bpha ligands connect the adjacent Co^{II} ions to result in a single-strand helix chain [Co-3-bpha]$_n$ with the Co···Co separation of 13.57 Å (Fig. 4b). The two carboxyl groups of MIP anions adopt chelate and monodentate coordination modes, respectively, to link the adjacent Co^{II} ions forming an infinite 1D [Co-MIP]$_n$ linear chain. The two types of 1D chains ([Co-3-bpha]$_n$ and [Co-MIP]$_n$) are alternatively connected with each other constructing 2D puckered (4,4) network (Fig. 4c). In addition, the adjacent 2D layers are interconnected by hydrogen-bonding interactions between the nitrogen atoms of 3-bpha ligands and oxygen atoms from MIP anions [N(3)–H(3B)···O(4), N···O = 3.073(9) Å] to generate the final 3D supramolecular framework (Fig. S4). Generally speaking, the "V"-shaped bis-pyridyl-bis-amide ligands tend to integrate with metal ions into ring-like structures, such as complexes **3** and **4** in this work and Zn(L)(bdc)·(H$_2$O)$_{0.5}$ in literature.[6d] While in complex **5**, the 3-bpha ligands connect Co^{II} ions to generate single-strand helix chains, which is rarely reported to our knowledge.

[Co$_3$(3-bpha)$_2$(1,3,5-BTC)$_2$(H$_2$O)$_4$]·2H$_2$O (6). Single crystal X-ray diffraction analysis reveals that **6** crystallizes in the orthorhombic system with space group *Pbcn*. The unit consists of three Co^{II} ions, two 3-bpha ligands, two 1,3,5-BTC anions, four coordinated water molecules and two lattice water molecules. There are two crystallographically independent Co^{II} centers. As shown in Fig. 5a, the Co1 center exhibits a {CoO_4} tetrahedral coordination geometry with four oxygen atoms from four 1,3,5-BTC anions [Co1–O = 2.013(5)–2.020(5) Å]. The Co2 ion shows a distorted octahedral coordination geometry, being coordinated by two pyridyl N atoms from two 3-bpha ligands [Co(2)–N(1) = 2.128(7) Å, Co(2)–N(4)#5 = 2.105(7) Å] and four oxygen atoms

CrystEngComm Accepted Manuscript

from one 1,3,5-BTC anion and two coordinated water molecules, respectively [Co2–O = 2.086(6)–2.206(6) Å].

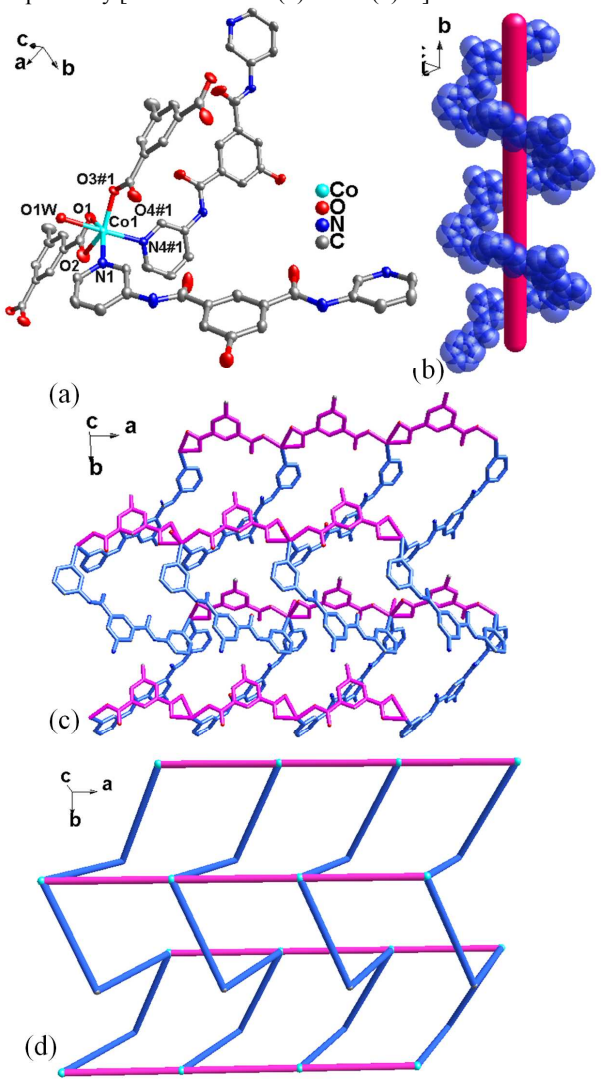

Fig. 4 (a) Coordination environment of the Co^{II} ion in **5** (#1 $x - 1$, y, z); (b) View of the 1D $[Co\text{-}3\text{-}bpha]_n$ helical chain; (c) The 2D network of **5**; (d) Simplification of the 2D structure to a 4–connected network. The hydrogen atoms are omitted for clarity.

In complex **6**, the carboxyl groups from 1,3,5-BTC anion exhibit two coordination modes: monodentate and chelate coordination modes. Two carboxyl groups of 1,3,5-BTC anion with monodentate mode linked the Co^{II} ions to generate a 2D sheet (Fig. 5b). The 3-bpha ligands adopt μ_2-bridging mode connecting adjacent Co^{II} ions to form a single-strand helix chain $[Co\text{-}3\text{-}bpha]_n$ (Fig. 5c). The 2D sheets and the 1D helix chains are further linked by the chelating carboxyl group of 1,3,5-BTC anions to form the final 3D framework (Fig. S5). In order to better understand the whole structure, the Co1/Co2 ions can be considered as 4-/3-connected nodes, the 1,3,5-BTC anions can be regarded as 3-connectors and the 3-bpha ligands can be viewed as linkers. So the structure of **6** can be simplified as a trinodal (3, 3, 4)-connected topology with the Schläfli symbol of $(8^3)_4(8^4{\cdot}10^2)$ (Fig. 5b). Sun *et al.* have reported a 2D network $[Co_3(L)_2(BTC)_2]{\cdot}4H_2O$ [17] [L = 3,3',5,5'-tetra(1H-imidazol-1-yl)-1,1'-biphenyl] based on the same metal and aromatic carboxylate ligand (1,3,5-BTC) with complex **6**, in which the Co^{II}-L 2D network is further linked by BTC anions resulting in the formation of final 2D structure. While in **6**, the BTC anions link the 2D sheets and the 1D helix chains to form a 3D framework. Thus, the N-donor ligands show significant effect on the final structures.

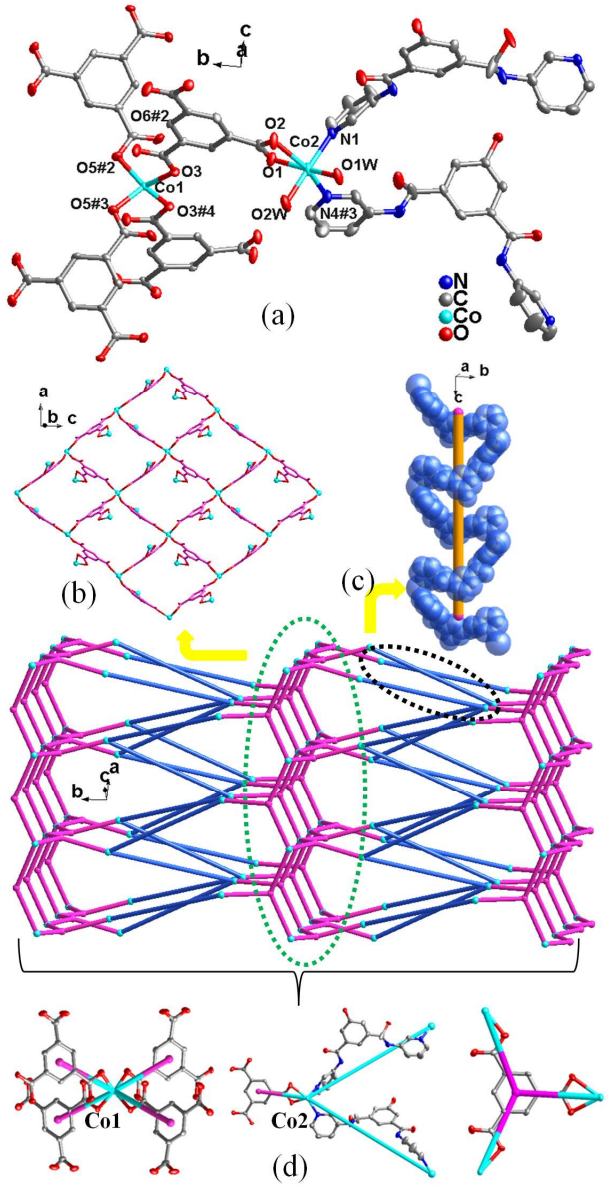

Fig. 5 (a) Coordination environment of the Co^{II} ion in **6** (#1 $-x + 3/2$, $-y + 1/2$, $z + 1/2$; #2 $x + 1/2$, $-y + 3/2$, $-z$; #3 $-x + 3/2$, $-y + 3/2$, $z - 1/2$; #4 $-x + 2$, y, $-z - 1/2$); (b) View of the 2D network; (c) View of the 1D $[Co\text{-}3\text{-}bpha]_n$ helical chain; (d) View of the 3D topology with $(8^3)_4(8^4{\cdot}10^2)$. The hydrogen atoms are omitted for clarity

Effect of the polycarboxylate anions on the structures of the title complexes

In this work, by tuning the polycarboxylate co-ligands with different carboxyl position and number as well as substitute groups under the same conditions, we obtained six new metal-organic complexes with different architectures. When a short pyridyl-containing dicarboxylate 2,3-H_2PDC was used in complex **1**, the 3-bpha ligand and 2,3-HPDC anion only act as the

CrystEngComm Accepted Manuscript

This journal is © The Royal Society of Chemistry [year]

terminal groups simultaneously with μ_1-coordination mode (Scheme 1) to coordinate with Co^{II} ion, resulting in the 0D complex **1**. The two oxygen atoms of –C=O groups from 3-bpha ligand are in the same orientation, the N···N (N1 and N4) distance of the terminal pyridyl group is 13.772(5) Å and the dihedral angles between the two pyridyl rings and benzene ring are 7.14° and 10.10°. When another nitro-containing dicarboxylate 3-H_2NPH was used instead of 2,3-H_2PDC in complex **2**, the 3-bpha ligand exhibits μ_2-bridging mode connecting the adjacent Co^{II} ions to form a 1D $[Co\text{-}3\text{-}bpha]_n$ meso-helical chain, and two carboxyl groups of each 3-NPH anion show a μ_1-η^1:η^1 chelating coordination mode to coordinate with Co^{II} ions as terminal groups. The oxygen atoms of –C=O groups from 3-bpha also turn the same orientation, the nitrogen-nitrogen (N1 to N4) distance of the 3-bpha ligand and the corresponding dihedral angles are 10.527(5) Å , 26.10° and 9.91°, respectively. When 1,3-H_2BDC and HIP were used in **3** and **4**, respectively, we obtained two similar structures. The 3-bpha ligands and dicarboxylates (1,3-BDC for **3** and HIP for **4**) in complexes **3** and **4** display the same coordination modes. The 3-bpha acting as bidentate ligands with μ_2-bridging mode integrate with Co^{II} ions to generate 28-membered $Co_2(3\text{-}bpha)_2$ rings. These $Co_2(3\text{-}bpha)_2$ loops connect adjacent 1D $[Co\text{-}1,3\text{-}BDC]_n$ chains in **3** and $[Co\text{-}HIP]_n$ in **4** to form the intricate 2D networks. The oxygen atoms of –C=O groups from 3-bpha in **3** and **4** are both in the opposite orientation. In complex **3**, the nitrogen atoms (N1 and N4) distance of the terminal pyridyl groups and the dihedral angles between the two pyridyl rings and benzene ring are 11.876(5) Å, 43.12° and 55.35°, respectively. While in complex **4**, the relative distance and dihedral angles are 10.926(5) Å, 17.94° and 18.41°, respectively. When a similar dicarboxylate MIP was selected in complex **5**, although the coordination mode of 3-bpha ligand is the same as that in complexes **3** and **4**, the μ_2-bridging 3-bpha ligands from **5** connect the adjacent Co^{II} ions to result in a single-strand helix chain $[Co\text{-}3\text{-}bpha]_n$, which is different from those in **3** and **4**. The adjacent $[Co\text{-}3\text{-}bpha]_n$ chains are connected by MIP anions to construct 2D puckered (4,4) network. The oxygen atoms of –C=O groups from 3-bpha in **5** turn the same orientation, the nitrogen-nitrogen (N1 to N4) distance of the 3-bpha ligand and the corresponding dihedral angles are 12.812(5) Å, 15.42° and 7.59°, respectively. In complexes **1**–**5**, all the Co^{II} ions adopt six-coordinated mode with octahedral coordination arrangement. When a tricarboxylate 1,3,5-BTC was used in complex **6**, the Co^{II} atoms exhibit six-coordinated and four-coordinated modes. The two carboxyl groups from 1,3,5-BTC anion with monodentate mode link the Co^{II} ions to generate a 2D sheet. The third carboxyl group of 1,3,5-BTC anion with a chelating coordination mode linked the single-strand helix $[Co\text{-}3\text{-}bpha]_n$ chains to form the final 3D framework. The oxygen atoms of –C=O groups turn the same direction. The N1···N4 distance of the 3-bpha ligand and the corresponding dihedral angles are 11.964(5) Å, 57.96° and 67.40°, respectively. The successful assembly of complexes **1**–**6** with different structures from 0D to 3D can be attributed to the effects of the polycarboxylate anions (Scheme 2). Therefore, we can conclude that both the substitute groups, position of carboxyl groups and carboxyl number of the polycarboxylates play significant roles in the construction and various architectures of the title complexes.

PXRD measurement and thermogravimetric analysis (TGA)

In order to confirm phase purity of the bulk materials for the title complexes, powder X-ray diffraction (PXRD) experiments were recorded. As shown in Fig. S7, the measured powder XRD patterns are in good agreement with the simulated ones, implying phase purities of the samples. The difference in reflection intensities between the simulated and experimental patterns may be attributed to the different orientation of the crystals in powder samples.[18]

To estimate the stability of the coordination architectures, the thermal behaviors of the title complexes were studied by TGA under N_2 atmosphere with a heating rate of 10 °C min^{-1} in the temperature range from room temperature to 800 °C (Fig. S8).

	Metal ion	Ligand	Carboxylic acid
1		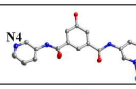	
2		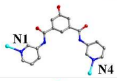	
3		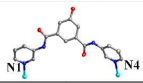	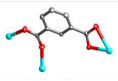
4		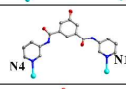	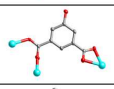
5		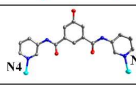	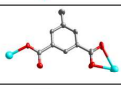
6	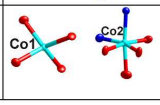	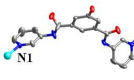	

Scheme 1 Coordination modes of Co^{II} ions, the 3-bpha ligand and polycarboxylates in complexes **1**–**6**.

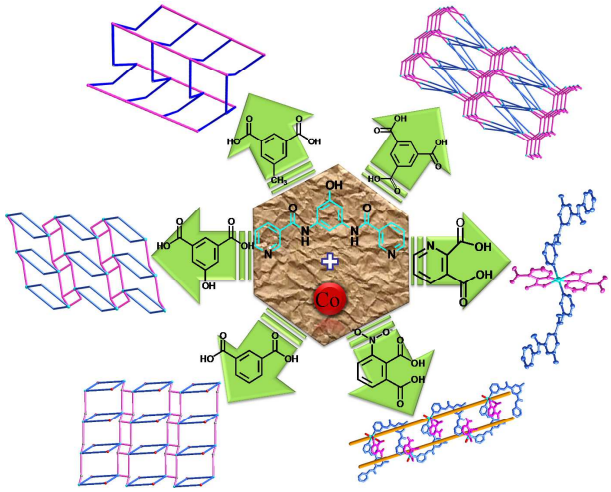

Scheme 2 Schematic view of the effect of polycarboxylates on the structures of complexes **1**–**6**.

The TG curves show that complex **1** displays only one weight loss step and complexes **2**–**6** exhibit two separate weight loss

CrystEngComm Accepted Manuscript

steps. In complex **1**, the weight loss is about 91.74% (calc. 92.92%) from 260 °C to 480 °C, corresponding to the decomposition of organic ligands, leading to the formation of CoO as the residue. The first weight loss stages are observed from 80 °C to 140 °C for **2**, 70 °C to 100 °C for **3**, 105 °C to 150 °C for **4**, 100 °C to 140 °C for **5**, 140 °C to 260 °C for **6**, giving the weight loss of about 9.12% for **2**, 13.11% for **3**, 7.53% for **4**, 4.21% for **5**, 8.32% for **6**, indicating the loss of the lattice water molecules or/and coordinated water molecules (calcd. 10.68% for **2**, 11.44% for **3**, 8.61% for **4**, 5.83% for **5**, 7.90% for **6**). The second weight loss starting at 190 °C up to 400 °C for **2**, 340 °C up to 470 °C for **3**, from 360 °C up to 510 °C for **4**, 350 °C up to 560 °C for **5**, 390 °C up to 550 °C for **6** may be due to the decomposition of 3-bpha and aromatic polycarboxylate ligands. The remaining weights are 10.09% for **2**, 8.93% for **3**, 10.12% for **4**, 11.23% for **5**, 15.97 for **6**, which can be assigned to CoO (calc. 11.12% for **2**,11.92% for **3**, 11.95% for **4**,12.35% for **5**, 16.45% for **6**).

Electrochemical behaviors of 1–6-CPEs

Redox properties of **1**–**6** were investigated in 0.01 M H_2SO_4 + 0.5 M Na_2SO_4 aqueous solution. The electrochemical behaviors of the **1**–**6**-CPEs are similar except for some slight potential shifts (Fig. S9 and Fig. 6). Thus, **2**-CPE is taken as an example to describe their cyclic voltammograms. As shown in Fig. 6, it can be seen clearly that a redox couple was observed in the potential range of +600 to -100 mV for **2**-CPE at different scan rates, which could be attributed to the redox of Co^{III}/Co^{II},[19] and the mean peak potential $E_{1/2} = (E_{pa} + E_{pc})/2$ is 264 mV (100 mV·s^{-1}). When the scan rates are varied from 20 to 300 mV s^{-1}, the peak potentials gradually change: the cathodic peak potentials shifted toward the negative direction and the corresponding anodic peak potentials shifted to the positive direction with increasing scan rates. In addition, the peak currents are proportional to the square-root of the scan rates up to 300 mV s^{-1} (inset of Fig. 6), which shows that the redox process of the **2**-CPE is diffusion-controlled.

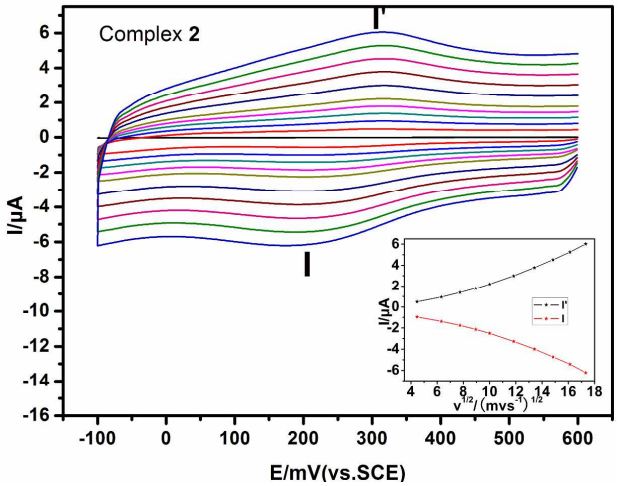

Fig. 6 Cyclic voltammograms of the **2**-CPE in 0.01 M H_2SO_4 + 0.5 M Na_2SO_4 aqueous solution at different scan rates (from inner to outer: 20, 40, 60, 80, 100, 140, 180, 220, 260, 300 mV s^{-1}). The inset shows the plots of the anodic and cathodic peak currents against the square-root of the scan rates.

Photocatalytic properties

Photocatalysts have attracted much attention because of their potential applications in purifying water by thoroughly decomposing organic pollutants.[20] Herein, the photocatalytic activities of complexes **1**–**6** were investigated with photodegradation of methylene blue (MB).[21] The photocatalytic reactions were performed through a typical process: 150 mg complex **1** or **2**, **3**, **4**, **5, 6** was mixed together with 90 mL aqueous solution of MB (10 mg·L^{-1}) under stirring in the dark for 30 min to ensure the equilibrium of the working solution. Then the solution was exposed to UV irradiation from an Hg lamp (125 W) and kept continuous stirring during irradiations. The samples of 5 mL were taken out every 30 min for analysis.

The absorption peaks of MB decrease obviously under UV irradiation in the presence of the title complexes, as shown in Fig. 7 and Fig. S10. The concentration of MB gradually decreases along with increasing of reaction time. The calculation results show that the conversion of MB is 72% for **1**, 52% for **2**, 57% for **3**, 55% for **4**, 56% for **5** and 49% for **6**, respectively (Fig. 8). It is obvious that the photocatalytic performance of complex **1** is the best one, which indicate that the difference of components and structure characters of the title complexes may influence their photocatalytic activities.[22] In addition, the control experiments on the degradation of MB were carried out in the following reaction conditions: (1) without catalyst; (2) complex **1** in the dark (Fig. S11). The results indicate that complexes **1**–**6** show photocatalytic activity for the degradation of MB, which may be candidates with photocatalytic activities in the degradation of some organic dyes.

As is known, on the photo-excitation of UV light, there is an electron transfer from the highest occupied molecular orbital (HOMO) contributed by oxygen and/or nitrogen 2p bonding orbital (valence band) to the lowest unoccupied molecular orbital (LUMO) contributed by empty metal orbital (conduction band). The HOMO strongly demands one electron to return to its stable state. Thus, one electron was captured from water molecule, which was oxygenated into the •OH radical. The •OH active species could decompose MB effectively to complete the photocatalytic process.[23]

Conclusion

We have successfully synthesized six new Co^{II} complexes from the mixed ligands of N,N′-bis(pyridin-3-yl)-5-hydroxybenzene-1,3-dicarboxamide and six different aromatic polycarboxylates under hydrothermal conditions. Complexes **1**–**6** show from 0D to 3D (0D for **1**, 1D for **2**, 2D for **3**, **4** and **5**, **3**D

CrystEngComm Accepted Manuscript

This journal is © The Royal Society of Chemistry [year]

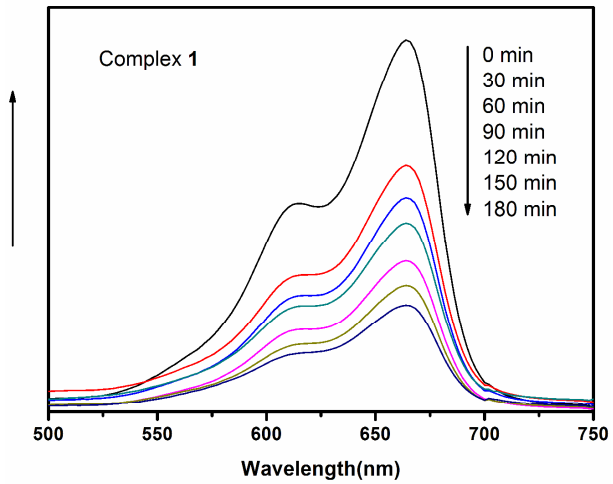

Fig. 7 Absorption spectra of the MB solution during the decomposition reaction under UV irradiation with the presence of complex **1**.

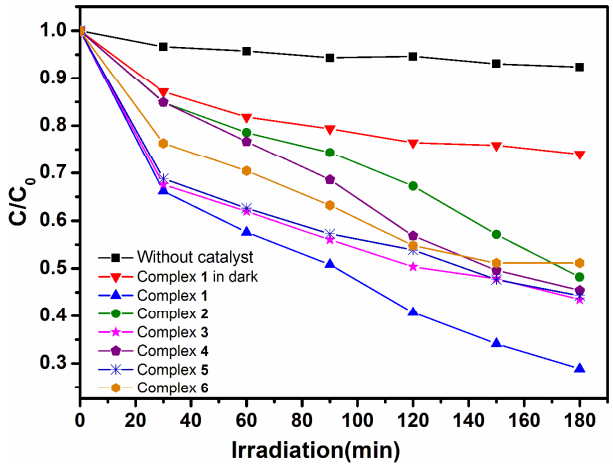

Fig. 8 Photocatalytic decomposition of MB solution under UV irradiation with the use of the title complexes, no catalyst under the same conditions and complex **1** in the dark.

for **6**) architectures, respectively. The polycarboxylates with different substitute groups, position of carboxyl groups and carboxyl number play important roles in the assembly and structures of the final complexes. Moreover complexes **1**–**6** display electrochemical properties and photocatalytic activities, demonstrating their possible potential applications in the catalysis and electrochemical fields.

Acknowledgements

This work was financially supported by the National Natural Science Foundation of China (No. 21171025, 21471021, 21401010) and Program of Innovative Research Team in University of Liaoning Province (LT2012020).

Notes and references

1 (a) J. P. Zhang, Y. Y. Lin, W. X. Zhang and X. M. Chen, J. Am. Chem. Soc., 2005, **127**, 14162; (b) M. Sorai, M. Nakano and Y. Miyazaki, Chem. Rev., 2006, **106**, 976; (c) L. Bastin, P. S. B arcia, E. J. Hurtado, J. A. C. Silva, A. E. Rodrigues and B. Chen, J. Phys. Chem. C, 2008, **112**, 1575; (d) W. Y. Gao, W. M. Yan, R. Cai, K. Williams, A. Salas, L. Wojtas, X. D. Shi and S. Q. Ma, Chem. Commun., 2012, **48**, 8898; (e) Z. L. Fang, J. G. He, Q. S. Zhang, Q. K. Zhang, X. Y. Wu, R. M. Yu and C. Z. Lu, Inorg. Chem., 2011, **50**, 11403; (f) N. C. Jeong, B. Samanta, C. Y. Lee, O. K. Farha and J. T. Hupp, J. Am. Chem. Soc., 2012, **134**, 51.

2 (a) K. L. Zhang, C. T. Hou, J. J. Song, Y. Deng, L. Li, S. W. Ng and G. W. Diao, CrystEngComm, 2012, **14**, 590; (b) G. Z. Liu, J. G. Wang and L. Y. Wang, CrystEngComm, 2012, **14**, 951; (c) F. J. Liu, D. Sun, H. J. Hao, R. B. Huang and L. S. Zheng, CrystEngComm, 2012, **14**, 379; (d) C. Ren, L. Hou, B. Liu, G. P. Yang, Y. Y. Wang and Q. Z. Shi, Dalton Trans., 2011, **40**, 793; (e) H. Wang, Y. Y. Wang, G. P. Yang, C. J. Wang, G. L. Wen, Q. Z. Shi and S. R. Batten, CrystEngComm, 2008, **10**, 1583.

3 X. L. Wang, Y. F. Bi, G. C. Liu, H. Y. Lin, T. L. Hu and X. H. Bu, CrystEngComm, 2008, **10**, 349.

4 (a) S. Hong, Y. Zou, D. Moon and M.S. Lah, Chem. Commun., 2007, **17**, 1707; (b) Z. Q. Qin, M. C. Jennings and R. J. Puddephatt, Chem. Eur. J., 2002, **8**, 735.

5 L. Luo, P. Wang, G. C. Xu, Q. Liu, K. Chen, Y. Lu, Y. Zhao and W. Y. Sun, Cryst. Growth Des., 2012, **12**, 2634.

6 (a) G. M. Sun, H. X. Huang, X. Z. Tian, Y. M. Song, Y. Zhu, Z. J. Yuan, W. Y. Xu, M. B. Luo, S. J. Liu, X. F. Feng and F. Luo, CrystEngComm, 2012, **14**, 6182; (b) S. Pandey, P. P. Das, A. K. Singh and R. Mukherjee, Dalton Trans., 2011, **40**, 10758; (c) J. Y. Lee, C. Y. Chen, H. M. Lee, E. Passaglia, F. Vizza and W. Oberhauser, Cryst. Growth Des., 2011, **11**, 1230; (d) G. M. Sun, Y, M. Song, Y, Liu, X. Z. Tian, H. X. Huang, Y. Zhu, Z. J. Yuan, X. F. Feng, M. B. Luo, S. J. Liu, W. Y. Xu and F. Luo, CrystEngComm, 2012, **14**, 5714; (e) J. W. Zhang, X. M. Kan, X. L. Li, J. Luan and X. L. Wang, CrystEngComm, 2015, **17**, 3887.

7 (a) X. L. Wang, J. Luan, H. Y. Lin, Q. L. Lu, C. Xu and G. C. Liu, Dalton Trans., 2013, **42**, 8375; (b) X. L. Wang, J. Luan, F. F. Sui, H. Y. Lin, G. C. Liu and C. Xu, Cryst. Growth Des., 2013, **13**, 3561.

8 (a) Y. Liang, F. K. Zhao, Q. L. Wang and Y. Y. Niu, J. Chem. Crystallogr., 2011, **41**, 763; (b) X. L. Wang, J. J. Huang, L. L. Liu, G. C. Liu, H. Y. Lin, J. W. Zhang, N. L. Chen and Y. Qu, CrystEngComm, 2013, **15**, 1960.

9 T. V. Mitkina, N. F. Zakharchuk, D. Y. Naumov, O. A. Gerasko, D. Fenske and V. P. Fedin, Inorg. Chem., 2008, **47**, 6748.

10 (a) J. W. Sun, M. T. Li, J. Q. Sha, P. F. Yan, C. Wang, S. X. Li and Y. Pan, CrystEngComm, 2013, **15**,10584; (b) H. H. Li, X. H. Zeng, H. Y. Wu, X. Jie, S. T. Zheng and Z. R. Chen, Cryst. Growth Des., 2014, **15**, 10.

11 M. Sarkar and K. Biradha, Cryst. Growth Des., 2006, **6**, 202.

12 T. Kuwana, W. G. French, Anal Chem, 1964, **36**, 241.

13 G. M. Sheldrick, Acta Crystallogr., Sect. A: Found. Crystallogr., 2008, **64**, 112.

14 A. L. Spek, PLATON, A Multipurpose Crystallographic Tool; Utrecht University: Utrecht, The Netherlands, 1998.

15 L. Wang, L. Ni and J. Yao, Polyhedron, 2013, **59**, 115.

16 X. L. Wang, J. Luan, H. Y. Lin, C. Xu and G. C. Liu, Inorg. Chim. Acta., 2013, **408**, 139.

17 L. Luo, G. C. Lv, P. Wang, Q. Liu, K. Chen and W. Y. Sun, CrystEngComm, 2013, **15**, 9537.

CrystEngComm Accepted Manuscript

18 X. Zhou, P. Liu, W. H. Huang, M. Kang, Y. Y. Wang and Q. Z. Shi, CrystEngComm, 2013, **15**, 8125.
19 T. V. Mitkina, N. F. Zakharchuk, D. Y. Naumov, O. A. Gerasko, D. Fenske and V. P. Fedin, Inorg. Chem., 2008, **47**, 6748.
20 B. Liu, Z. T. Yu, J. Yang, W. Hua, Y. Y. Liu and J. F. Ma, Inorg. Chem., 2011, **50**, 8967.
21 Y. Hu, F. Luo and F. F. Dong, Chem. Commun., 2011, **47**, 761.
22 (a) H. S. Lin and P. A. Maggard, Inorg. Chem., 2008, **47**, 8044; (b) W. Q. Kan, B. Liu, J. Yang, Y. Y. Liu and J. F. Ma, Cryst. Growth Des., 2012, **12**, 2288; (c) A. K. Paul, R. Karthik and S. Natarajan, Cryst. Growth Des., 2011, **11**, 5741.
23 (a) Y. Q. Chen, S. J. Liu, Y. W. Li, G. R. Li, K. H. He, Y. K. Qu, T. L. Hu and X. H. Bu, Cryst. Growth Des., 2012, **12**, 5426; (b) J. X. Meng, Y. Lu, Y. G. Li, H. Fu and E. B. Wang, CrystEngComm, 2011, **13**, 2479; (c) J. Guo, J. Yang, Y. Y. Liu and J. F. Ma, CrystEngComm, 2012, **14**, 6609; (d) H. X. Yang, T. F. Liu, M. N. Cao, H. F. Li, S. Y. Gao and R. Cao, Chem. Commun., 2010, **46**, 2429.

CrystEngComm Accepted Manuscript

This journal is © The Royal Society of Chemistry [year]

Polycarboxylate-directed various Co(II) complexes based on a "V"-like bis-pyridyl-bis-amide derivative: Construction, electrochemical and photocatalytic properties

Xiu-Li Wang*, Xiao-Ting Sha, Guo-Cheng Liu, Nai-Li Chen and Yuan Tian

Six Co^{II} complexes have been hydrothermally synthesized using a "V"-like N,N′-bis(pyridin-3-yl)-5-hydroxybenzene-1,3-dicarboxamide as the main ligand and six polycarboxylates as the auxiliary ligands. The effects of the polycarboxylates on the structures of the title complexes have been discussed.

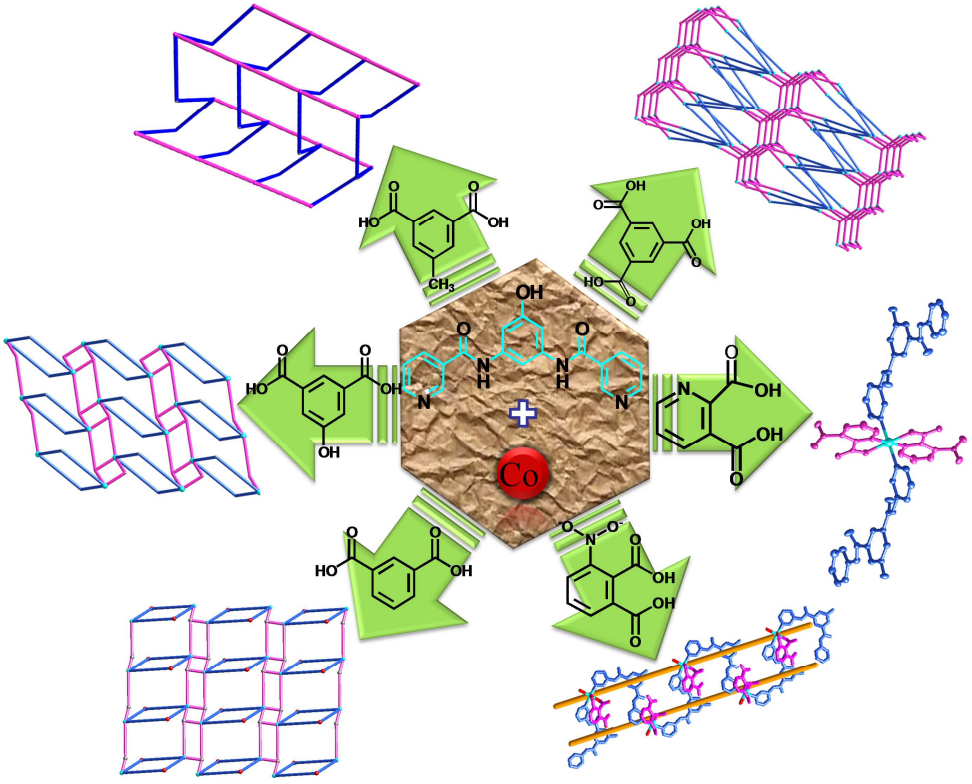

∗ Corresponding author. Tel.: +86-416-3400158

E-mail address: wangxiuli@bhu.edu.cn (X.-L. Wang)

CrystEngComm Accepted Manuscript